Diagnosis of Glioblastoma by Immuno-Positron Emission Tomography

Subjects: Oncology

Contributor: Alberto J. Schuhmacher

Resonance Imaging (MRI) is the most widely used non-invasive technique in the primary diagnosis of glioblastoma. Although MRI provides very powerful anatomical information, it has proven to be of limited value for diagnosing glioblastomas in some situations. The final diagnosis requires a brain biopsy that may not depict the high intratumoral heterogeneity present in this tumor type. The gold standard tracer for most PET cancer imaging is 2-[18F]fluoro-2-deoxy-D-glucose ([18F]FDG), a fluorine-18 glucose analog, being the most widely used in clinical radiopharmaceutical practice, and accounting for more than 90% of total PET scans. [18F]FDG is ineffective for diagnosing gliomas due to the high glucose metabolism in the normal brain, which results in suboptimal tumor detection and delineation, especially upon treatment. An innovative option for biomarker identification in vivo is termed “immunotargeted imaging”. By merging the high target specificity of antibodies with the high spatial resolution, sensitivity, and quantitative capabilities of positron emission tomography (PET), “Immuno-PET” allows us to conduct the non-invasive diagnosis and monitoring of patients over time using antibody-based probes as an in vivo, integrated, quantifiable, 3D, full-body “immunohistochemistry” in patients.

Keywords: diagnostic imaging ; immuno-PET ; glioblastoma ; neuroimaging ; molecular imaging ; antibody ; nanobody ; theragnostic probes

1. Introduction

Glioblastoma is the most common and aggressive tumor of the central nervous system in adults [1]. With an incidence of 3.23 cases per 100,000 individuals in Europe and the USA, glioblastoma represents ~49.1% of primary malignant brain tumors [1][2]. Despite continuous advances in the molecular classification of glioblastoma, and the steady progress in surgical, radiological, and chemotherapeutic treatment options [1][3][4], patient survival has improved only marginally during the past 3 decades. Current glioblastoma survival rates average just 8–14.6 months, with only ~5% of patients surviving more than 5 years [1][5]. Recurrence of glioblastoma is nearly universal and is associated with poor prognosis; patients with recurrent glioblastoma have a median survival of only 5–7 months with optimal therapy [6].

The current standard-of-care for treatment of newly diagnosed glioblastoma has remained relatively unchanged since 2005 and consists of maximal safe resection followed by concomitant chemoradiation with the alkylating agent temozolomide (TMZ), and subsequent adjuvant TMZ [7].

The DNA-repair enzyme O^6-methylguanine-DNA methyltransferase (MGMT) impairs the killing of tumor cells by alkylating agents chemotherapy [8]. Methylation of the *MGMT* promoter regulates its expression. Despite confirming the prognostic significance of *MGMT* promoter methylation, survival did not improve with TMZ [9].

In 2011, a novel therapeutic approach, the first-generation tumor treating fields (TTF) device, was approved by the Food and Drug Administration (FDA) for the treatment of recurrent glioblastoma [10]. The TTF device was subsequently approved as adjuvant therapy for newly-diagnosed glioblastoma in 2015 [10][11].

2. Current Status of Glioblastoma Classification and Diagnosis

The 2016 World Health Organization (WHO) Classification of Tumors of the Central Nervous System (WHO CNS4) incorporated for the first time genetic alterations into the classification system to create more homogenous disease categories with greater prognostic value [12]. The WHO CNS4 classification symbolized a paradigm shift, replacing classical histology-based glioma diagnostics with an integrated histological and molecular classification system that enables more precise tumor categorization [12][13]. The incorporated diagnostic biomarkers in the 2016 WHO classification

of gliomas were Isocitrate dehydrogenase (*IDH*)-*1/2* mutations, 1p/19q codeletion, H3 Histone, Family 3A (*H3F3A*) or HIST1H3B/C K27M (*H3-K27M*) mutations, and *C11orf95–RELA* fusions [13].

The novel 2021 classification (WHO CNS5) moves further to advance the role of molecular diagnostics in CNS tumor classification but stills remains rooted in other established approaches to tumor characterization, including histology and immunohistochemistry [14]. The WHO CNS5 assumes that most tumor types are aligned to distinct methylation profiles [15]. While these are not specified in every tumor definition, the information about diagnostic methylation is included in the "Definitions" and "Essential and Desirable Diagnostic Criteria" sections of WHO CNS5 and could provide more critical guidance for diagnosis [14].

WHO CNS5 considers all IDH mutant diffuse astrocytic tumors as "Astrocytoma, IDH-mutant" and are then graded as CNS WHO grade 2, 3, or 4. Furthermore, grading is no longer entirely histological, since the presence of CDKN2A/B homozygous deletion results in a CNS WHO grade of 4, even in the absence of microvascular proliferation or necrosis [14].

For a diagnosis of "Glioblastoma, IDH-wildtype" the novel WHO CNS5 incorporates 3 genetic parameters (*TERT* promoter mutation, *EGFR* gene amplification, combined gain of entire chromosome 7 and loss of entire chromosome 10) as criteria. For IDH-wildtype diffuse astrocytic tumors in adults, several works have shown that the presence of 1 or more of the 3 genetic parameters is sufficient to assign the highest WHO grade [16][17]. Consequently, "Glioblastoma, IDH-wildtype" in adults should be diagnosed in the setting of an IDH-wildtype diffuse and astrocytic glioma if there is either microvascular proliferation, or necrosis, or *TERT* promoter mutation, or *EGFR* gene amplification, or +7/−10 chromosome copy number changes. In IDH-wildtype diffuse astrocytomas occurring in younger age groups, however, consideration should be given to the different types of diffuse pediatric-type gliomas [14].

3. Neuroimaging

Neuroimaging has transformed neuro-oncology and the way glioblastoma is diagnosed and treated. First, with the advent of Computed Tomography (CT), and subsequently the Magnetic Resonance Imaging (MRI), these technologies have permitted an earlier identification of asymptomatic lesions. Nowadays, imaging is critical for pre-surgical diagnosis, intraoperative management, surgery, and ultimately monitoring after treatment with radiation and chemotherapy [18]. Anatomic imaging remains critical to identifying glioblastomas, but increasingly, advanced imaging methods allowing physiologic imaging have impacted the way these patients are managed [18].

4. Elements of Immuno-PET: Target, Antibody and Radionuclide

We live within a "cancer-omics" revolution that reveals many clinically relevant alterations that are not yet included into the medical practice, at least partly due to the limited number of non-invasive imaging biomarkers [19]. An innovative option, termed "immunotargeted imaging", merges the target specificity and selectivity of antibodies and derivatives towards a given tumor cell surface marker with the capabilities of a given imaging technique. Immunotargeted imaging by PET necessitates three components that are required to fulfill several characteristics: a suitable target for imaging, an optimally engineered antibody for imaging applications, and selecting an appropriate radionuclide for immuno-PET (**Figure 1**).

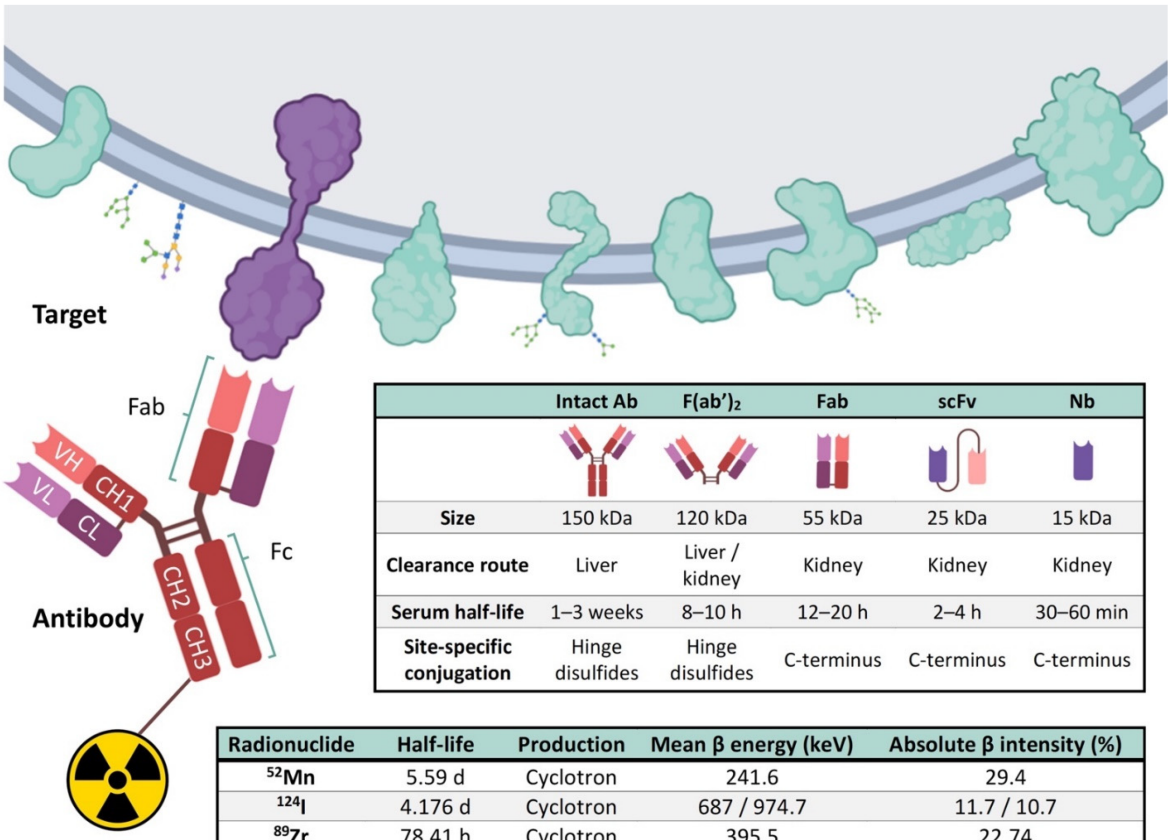

	Intact Ab	F(ab')$_2$	Fab	scFv	Nb
Size	150 kDa	120 kDa	55 kDa	25 kDa	15 kDa
Clearance route	Liver	Liver / kidney	Kidney	Kidney	Kidney
Serum half-life	1–3 weeks	8–10 h	12–20 h	2–4 h	30–60 min
Site-specific conjugation	Hinge disulfides	Hinge disulfides	C-terminus	C-terminus	C-terminus

Radionuclide	Half-life	Production	Mean β energy (keV)	Absolute β intensity (%)
^{52}Mn	5.59 d	Cyclotron	241.6	29.4
^{124}I	4.176 d	Cyclotron	687 / 974.7	11.7 / 10.7
^{89}Zr	78.41 h	Cyclotron	395.5	22.74
^{76}Br	16.2 h	Cyclotron	1532	25.8
^{86}Y	14.74 h	Cyclotron	535.4	11.9
^{64}Cu	12.7 h	Cyclotron	278.2	17.6
^{44}Sc	3.97 h	Generator	632.0	94.27
^{18}F	109.77 min	Cyclotron	249.8	96.73
^{68}Ga	67.7 min	Generator	836	87.72

Figure 1. Representation of the three main components of the immuno-PET. Targets present in the external surface of the plasma membrane, antibody, and its derived immune fragments F(ab')$_2$, Fab, scFv, and Nb, and the most commonly used radionuclides are represented. A typical antibody (Immunoglobulin G, IgG) is composed of two heavy (H) chains and 2 light (L) chains. Heavy chains contain a series of immunoglobulin domains, usually with one variable domain (VH) that is important for antigen binding, and several constant domains (CH1, CH2, CH3). Light chains are composed of one variable (VL) and one constant (CL) domain. Abbreviations: Variable (V) and constant (C), Light (L), and Heavy (H); Ab, Antibody; Fab, Fragment antigen-binding; F(ab')$_2$,Fab dimer; scFv, single-chain variable fragment; Nb, Nanobody; ^{18}F, Fluorine; ^{44}Sc, Scandium; ^{52}Mn, Manganese; ^{64}Cu-Copper; ^{68}Ga, Gallium; ^{76}Br, Bromine; ^{86}Y, Yttrium; ^{89}Zr, Zirconium; ^{124}I, Iodine [20][21][22]. Figure adapted with permission from Gónzalez-Gómez et al. [23]. Image created with BioRender.com (accessed on 6 September 2021).

5. Current Perspectives of Immuno-PET for Glioblastoma

Several targets are functionally relevant in glioblastoma, since they have clinical potential as prognostic markers. In addition, they could be used as molecular targets for the delivery of agents for their detection. To date, immuno-PET imaging probes have been mainly designed to target glioblastoma tumors in preclinical models. Several of them have already been successful in detecting gliomas in preclinical studies, as shown in **Table 1**. These tracers allow for evaluating multiple hallmarks [24] of gliomas and the treatment response in preclinical settings.

Table 1. Immune-PET tracers for glioblastoma.

PET Imaging Probes	Conjugation Strategy	Targets	Application	Models	References
[^{18}F]AlF-NOTA/NODAGA-PODS-Z-EGFR:03115 (EGFR-targeting affibody molecule)	Cysteine-based random	EGFR	Many EGFR gene alterations have been identified in gliomas, especially glioblastomas.	Subcutaneous xenograft mouse model with U-87 MG vIII cells	[25]
[^{124}I]I-PEG$_4$-tptddYddtpt-ch806 (tptddYddtpt is a peptide ‘‘clicked’’ onto dibenzyl-clooctyne(DBCO)-derivatized ch806)	Click chemistry	EGFR	ch806, an anti-EGFR mAb, can distinguish tumor cells with an amplified/overexpressed EGFR phenotype from normal cells having wild-type levels of EGFR expression.	Subcutaneous xenograft mouse model with U-87 MG.de2-7 cells	[26]
[^{44}Sc]Sc−CHX-A″-DTPA−Cetuximab-Fab	Lysine-based random	EGFR	Radiolabeling and preclinical evaluation of ^{44}Sc-labeled protein molecules.	Subcutaneous xenograft mouse model with U-87 MG	[27]
[^{89}Zr]Zr-DFO-cetuximab	Lysine-based random	EGFR	^{89}Zr-cetuximab was used to assess transient BBB disruption in vivo permeability induced by the combination of injected microbubbles with low intensity focused ultrasound.	Orthotopic murine glioma with GL261 cells	[28]
[^{64}Cu]Cu-NOTA-Bs-F(ab)$_2$ (bispecific immunoconjugate by linking two antibody Fab……fragments, an anti-EGFR and an anti-CD105)	Lysine-based random	EGFR and CD105	EGFR has been extensively studied as a target for anticancer therapy, and its activation stimulates tumor proliferation and angiogenesis. Similarly, CD105 (also called endoglin) is abundantly expressed on activated endothelial cells, and such over-expression is an adverse prognostic factor in many malignant tumor types.	Subcutaneous xenograft mouse model with U-87 MG	[29]
[^{64}Cu]Cu-NOTA-EphA2-4B3 (human anti-EphA2 mAb)	Lysine-based random	EphA2	EphA2 receptor tyrosine kinase is overexpressed in several tumors, including glioblastoma.	Orthotopic brain glioblastoma murine models (two patient-derived cell lines and U-87 MG cells)	[30]

PET Imaging Probes	Conjugation Strategy	Targets	Application	Models	References
[^{89}Zr]Zr-DFO-mCD47	Lysine-based random	CD47	CD47 is a membrane protein overexpressed on the surface of most cancer cells. It is involved in the increase in intracellular [Ca^{2+}] that occurs upon cell adhesion to the extracellular matrix and is also a receptor for the C-terminal cell-binding domain of thrombospondin.	Orthotopic murine glioma with GL261 cells	[31]
[^{64}Cu]Cu-NOTA-AC133 (anti-AC133 mAb)	Lysine-based random	AC133	AC133 is an N-glycosylation-dependent epitope of the second extracellular loop of CD133/prominin-1, a cholesterol-binding protein of unknown function that locates to plasma membrane protrusions. $AC133^{+}$ tumor stem cells have been described for glioblastoma multiforme.	Orthotopic and subcutaneous xenograft mouse models with NCH421k and U-251 MG cells	[32]
[^{89}Zr]Zr-DFO-bevacizumab (humanized anti-VEGF)	Lysine-based random	VEGF	^{89}Zr-labeled bevacizumab was used to assess BBB opening with mannitol.	C3HeB/FeJ mice without tumors	[33]
[^{68}Ga]Ga-DOTA-bevacizumab (humanized anti-VEGF)	Lysine-based random	VEGF	^{68}Ga-labeled bevacizumab was used to assess BBB opening with focused ultrasound exposure in the presence of microbubbles.	Orthotopic murine glioma with U-87 MG cells	[34]
[^{89}Zr]Zr-DFO-YY146 (anti-CD146 mAb)	Lysine-based random	CD146	CD146 plays an important role in several processes involved in tumor angiogenesis, progression, and metastasis. Its expression has been correlated with aggressiveness in high-grade gliomas.	Subcutaneous xenograft mouse model with U-87 MG and U251 cells	[35]
[^{64}Cu]Cu-NOTA-YY146 (anti-CD146 mAb)	Lysine-based random	CD146	CD146 plays an important role in several processes involved in tumor angiogenesis, progression, and metastasis. Its expression has been correlated with aggressiveness in high-grade gliomas.	Orthotopic and subcutaneous xenograft mouse models with U-87 MG and U-251 MG cells	[36]

PET Imaging Probes	Conjugation Strategy	Targets	Application	Models	References
[^{64}Cu]Cu-NOTA-61B (human anti-Dll4 mAb)	Lysine-based random	DII4	DII4 plays a key role to promote the tumor growth of numerous cancer types.	Subcutaneous xenograft mouse model with U-87 MG	[37]
[^{89}Zr]Zr-DFO-LEM2/15 (anti-MM1-MMP mAb)	Lysine-based random	MT1-MMP/ MMP14	MMP14 is a metalloprotease frequently overexpressed in many tumors, and it is associated with tumor growth, invasion, metastasis, and poor prognosis.	Xenograft mice bearing human U251 cells and two orthotopic brain glioblastoma murine models (patient-derived TS-543 neurospheres and U-251 MG cells)	[38]
[^{89}Zr]Zr-DFO-fresolimumab (human IgG4 mAb, 1D11)	Lysine-based random	TGFβ	TGFβ mediates extracellular matrix (ECM) remodeling, angiogenesis, and immunosuppression, and regulates tumor cell motility and invasion.	Orthotopic murine glioma with GL261 and SB28 cells	[39]
[^{89}Zr]Zr-DFO-fresolimumab (human IgG4 mAb, 1D11)	Lysine-based random	TGFβ	TGFβ mediates ECM remodeling, angiogenesis, and immunosuppression, and regulates tumor cell motility and invasion.	Patients with recurrent high-grade glioma	[40]
[^{89}Zr]Zr-DFO-F19 (anti-FAP monoclonal antibody)	Lysine-based random	FAP	FAP, a 170 kDa type II transmembrane serine protease, is expressed on glioma cells and within the glioma tumor microenvironment.	Subcutaneous xenograft mouse model with U-87 MG cells	[41]
[^{89}Zr]Zr-DFO-PD-1	Lysine-based random	PD-1	^{89}Zr labeled αPD-1 antibody was used to assess focal BBB permeability induced by high-intensity, focused ultrasound.	Orthotopic murine glioma with G48a cells	[42]
[^{68}Ga]Ga-NOTA-Nb109 (anti-PD-L1 nanobody)	Lysine-based random	PD-L1	Evaluate the specific affinity of 68Ga-NOTA-Nb109 to several cancer cell lines that expressed endogenous PD-L1.	Subcutaneous xenograft mouse model with U-87 MG cells	[43]

PET Imaging Probes	Conjugation Strategy	Targets	Application	Models	References
[^{89}Zr]Zr-DFO-169 cDb (anti-CD8 cys-diabody)	Lysine-based random	CD8	Proof-of-concept to detect CD8+ T cell immune response to oncolytic herpes simplex virus (oHSV) M002 immunotherapy in a syngeneic glioblastoma model.	Orthotopic syngeneic murine glioma with GSC005 cells	[44]
[^{89}Zr]Zr-DFO-CD11b	Lysine-based random	CD11b	The most abundant population of immune cells in glioblastoma is the CD11b^{+} tumor-associated myeloid cells.	Mice bearing established orthotopic syngeneic GL261 gliomas	[45]
[^{89}Zr/^{177}Lu]Zr/Lu-Lumi804-CD11b	Lysine-based random	CD11b	Theragnostic approach for monitoring and reducing tumor-associated myeloid cells in gliomas to improve immunotherapy responses.	Mice bearing established orthotopic syngeneic GL261 gliomas	[46]
[^{89}Zr]Zr-DFO-OX40	Lysine-based random	CD134	CD134 (or OX40) is an activated T-cell surface marker, known to be a costimulatory transmembrane molecule of TNF superfamily, primarily expressed on activated effector T cells and regulatory T cells.	Mice bearing established orthotopic GL261 gliomas	[47]

Abbreviations: CD8—Cluster of differentiation 8; CD11b—Integrin αM; CD47—Cluster of differentiation 47; CD105—endoglin; CD134—Tumor necrosis factor receptor superfamily, member 4 (TNFRSF4); CD146—Cluster of Differentiation 146; DLL4—Delta-Like Ligand 4; EGFR—Epidermal Growth Factor Receptor; EPHA2—Ephrin type-A receptor 2; FAP—Fibroblast activation protein alpha; MT1-MMP/MMP14—Membrane-type 1 matrix metalloproteinase; PD-1—programmed cell death receptor-1; PD-L1—Programmed cell death ligand 1; TGFβ—Transforming growth factor β; VEGF—Vascular Endothelial Growth Factor.

Several immuno-PET tracers' [25][26][27][28][29][30][31][32][37][38] target membrane proteins whose expression is altered in glioblastoma including the Epidermal Growth Factor Receptor (EGFR), Delta-Like Ligand 4 (DLL4), Ephrin type-A receptor 2 (EPHA2), Cluster of differentiation 47 (CD47), the AC133 antigen, and the Membrane-type 1 matrix metalloproteinase (MT1-MMP/MMP14). In vivo administration of these tracers showed high-specific-contrast imaging of the target in an MT1-MMP expressing glioblastoma tumor model and provided strong evidence for their utility as an alternative to non-specific imaging of glioblastoma

Glioblastomas develop in complex tissue environments, which support sustained growth, invasion, progression, and response to therapies [48]. Several components of the tumor microenvironment such as vessels [39][40][41], macrophages, and extracellular matrix proteins [35][36] are also promising candidates for the development of immuno-PET diagnostic approaches in glioblastoma [39][40][41][45].

Re-education of the tumor microenvironment of glioblastomas emerges as a novel opportunity for therapeutic intervention, as it has anti-tumorigenic effects [49][50].

Macrophages and microglia accumulate with glioblastoma progression and can be targeted via inhibition of Colony-Stimulating Factor-1 Receptor (CSF-1R) to regress high-grade tumors in animal models of glioblastoma [49][50]. A recent immuno-PET tracer targeting the Integrin αM (CD11b) expressing cells (macrophages) with high specificity in a mouse

model of glioblastoma was developed, demonstrating the potential for non-invasive quantification of tumor-infiltrating CD11b+ immune cells during disease progression and immunotherapy in patients suffering of glioblastoma [30][45]. Another anti-CD11b tracer has been shown to be effective in mouse models for imaging tumor-associated myeloid cells (TAMCs), which constitute up to 40% of the cell mass of gliomas [46].

Immunotherapy, especially immune-checkpoint inhibitors, is transforming oncology. Despite glioblastomas frequently express the programmed cell death ligand 1 (PD-L1), the results obtained with anti-PD1 therapy are below expectations. The frequent intratumor variability of PD-L1 expression carries significant implications for determination accuracy. PET imaging of immune-checkpoint inhibitors may serve as a robust biomarker to predict and monitor responses to these immunotherapies, complementing the existing immunohistochemical techniques [51].

Other immuno-PET tracers targeting immune cells have been evaluated. A tracer targeting CD8+ T cell immune response to oncolytic herpes simplex virus (oHSV) M002 immunotherapy was evaluated as a proof of concept in a syngeneic glioblastoma model [44]. Another monoclonal antibody-based tracer was developed for immuno-PET imaging of T-cell activation targeting the costimulatory receptor OX40, and used to monitor the stimulated T-cell response in a murine orthotopic glioma model [47].

Furthermore, some of these immuno-PET tracers are valuable tools to determine the transient BBB disruption and permeability induced by mannitol [33] or produced by the combination of injected microbubbles with low-intensity focused ultrasound in vivo [28][34][42]. Notably, [^{89}Zr]Zr-DFO-fresolimumab, an immuno-PET tracer based on a monoclonal antibody that can neutralize all mammalian isoforms of TGF-β, was assayed in humans and penetrated recurrent high-grade gliomas but did not result in clinical benefit [40].

6. Novel Nanobody-Based Immuno-PET Imaging Methods for Glioblastoma

The development of immuno-PET probes for the diagnosis of glioblastoma may encounter several hurdles to be reached due to the intracranial location of this tumor type. CNS barriers may limit the delivery of conventional antibody-based immuno-PET probes. The restricted entrance of molecules into the CNS is exerted mainly by the blood–brain barrier (BBB) and the blood–cerebrospinal fluid (CSF) barrier (BCSFB) [52]. These dynamic interfaces allow the exclusive passage from the blood into the CNS of receptor-specific ligands and small molecules (MW < 400 Da) that are lipid-soluble [53][54]. The delivery of peptide and protein drugs through the BBB is a major challenge for treating CNS diseases, and strategies to achieve therapeutic concentrations are under development [55]. In this regard, only 0.01–0.4% of the total amount of administered therapeutic antibodies have access to the CNS through passive diffusion [56][57]. Transport of therapeutic antibodies, mostly with the IgG isotype (150 kDa), may be hampered by the binding of their Fc domain to Fc receptors in the BBB [58]. Both the Fcγ receptor (FcγR) and neonatal Fc receptor (FcRn) have been implicated in the inverse transport of IgG through the BBB and their subsequent return from the brain to blood circulation [59][60]. Nevertheless, recent studies have proposed that antibody transcytosis across the BBB is carried by non-saturable, non-specific, Fc-independent mechanisms [61]. These mechanisms may hinder the diagnostic potential of monoclonal antibody-based immune-PET tracers for glioblastoma patients.

The development of antibody subunits targeting glioblastoma biomarkers that overcome the BBB selectivity emerges as a promising tool that could contribute to glioblastoma diagnosis by immuno-PET [62]. Single-domain antibodies (sdAbs) such as nanobodies have a lower MW, enabling better BBB penetrance, tumor uptake, and faster blood clearance than monoclonal antibodies [63][64]. Nanobodies are the single variable domain of the heavy-chain-only antibodies of *Camelidae* (camel, dromedary, llama, alpaca, vicuñas, and guananos) [65][66]. Nanobodies constitute the smallest molecules derived from antibodies (diameter of 2.5 nm and height of 4 nm; 15 kDa), although they still conserve full antigen-binding capacity with high specificity and affinity [67]. Nanobodies exert low toxicity and immunogenicity. Nanobodies have demonstrated their potential utility in diagnosing, monitoring, and therapy of a wide range of diseases [68][69]. Several differentially expressed proteins have been identified as glioblastoma targets with potential tumor-class predictive biomarker values [70][71]. Furthermore, a wide range of nanobodies targeting glioblastoma targets that have shown cytotoxic effects might constitute potential candidates for developing nanobody-based molecular imaging probes. Candidate nanobodies for immuno-PET approaches recognize molecular targets which play important roles in protein biosynthesis (TUFM, TRIM28), DNA repair and cell cycle (NAP1L1), and cellular growth and maintenance (EGFR, DPYSL2, β-Actin) [72][73][74]. Recently, a PD-L1-targeting nanobody-based tracer was evaluated to assess the changes in PD-L1 expression sensitively and specifically in different cancer types, which could help screen patients with high expression and guide PD-L1-targeting immunotherapies (**Table 1**) [43].

In contrast to conventional antibodies, nanobody-based immuno-PET probes may launch a novel era for the diagnosis of glioblastoma. Various molecular mechanisms for the transportation of nanobodies through the BBB have been extensively described [75][76][77][78] (**Figure 2**). Receptor-mediated transcytosis performs the movement of receptor ligands (e.g., transferrin, lactoferrin) across the BBB by a specific affinity-dependent unidirectional transport [79][80]. Nanobody FC5 (GenBank no. AF441486), the first nanobody described to traverse the BBB, binds the alpha(2,3)-sialoglycoprotein receptor in the brain endothelium [81][82]. FC5 set the basis for delivering BBB-impermeable therapeutic agents into the brain parenchyma by exploiting the receptor-mediated transcytosis of nanobodies [83]. Adsorptive-mediated transcytosis triggers the transport of basic molecules by electrostatic interactions with anionic microdomains on the cell membrane [84][85]. Several nanobodies with high isoelectric points (pI~9.5) have reported spontaneous delivery into the brain parenchyma. Basic nanobodies mVHH E9 (pI = 9.4), R3VQ (pI > 8.3), and A2 (pI > 9.5) have been shown to traverse the BBB and specifically label their molecular brain targets in vivo [86][87]. Transcytosis of nanobodies may be improved by other molecular shuttles such as peptide-decorated liposomes and cell-penetrating peptides (CPPs), which interact with the endothelial cells of the BBB and undergo nanobody internalization into the brain parenchyma [88][89][90].

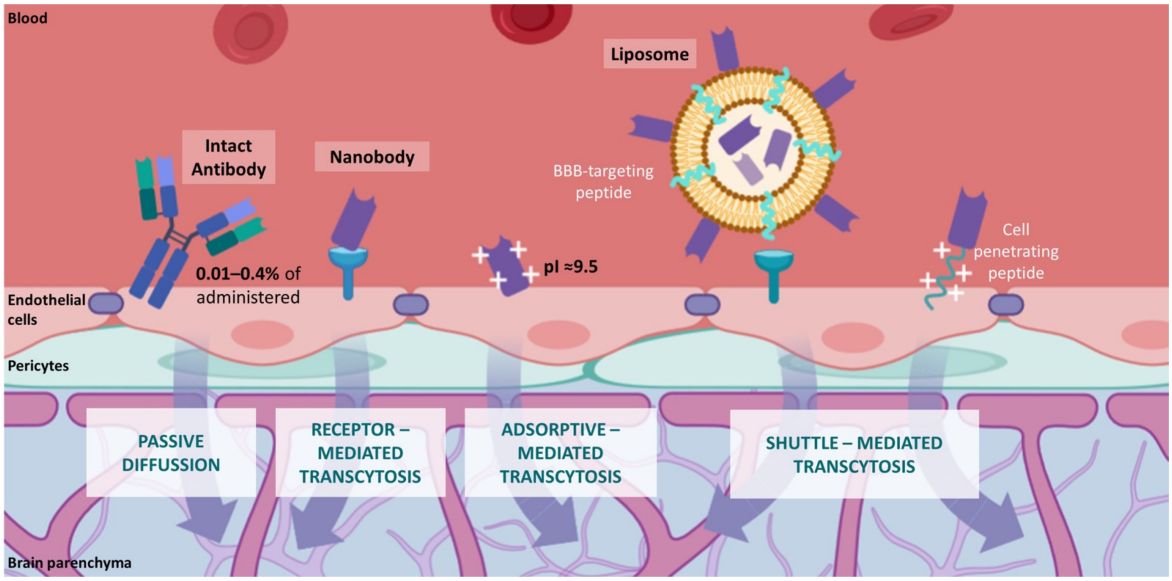

Figure 2. Molecular mechanisms of BBB permeability to antibodies. Comparison of conventional IgG antibodies (passive diffusion) and nanobodies (transcytosis mediated by BBB receptors, adsorptive processes, and BBB shuttle molecules). Image created with BioRender.com (accessed on 6 September 2021).

In this regard, nanobodies crossing the BBB can be utilized as the targeting moieties of diagnostic and/or therapeutic immuno-PET tracers for CNS diseases. Nanobodies have already been used as non-invasive probes in several imaging techniques to visualize molecular pathologies, including glioblastoma [91]. First attempts labeled nanobodies with fluorescent dyes to perform in vivo optical imaging. The named EG2 nanobody and its bivalent (EG2-hFc) and pentavalent (V2C-EG2) formats were conjugated to the near-infrared (NIR) Cy5.5 fluorophore and successfully detected EGFRvIII expressing tumors in orthotopic mouse models of glioblastoma by NIR fluorescence imaging [92]. Similar results were obtained with the derivative nanobody EG2-Cys, labeled with NIR quantum dot Qd800 [93]. Cy5.5-labeled VHH 4.43, a nanobody directed against insulin-like growth factor-binding protein 7 (IGFBP7), was able to selectively detect blood vessels of glioblastoma after systemic injection in orthotopic glioblastoma bearing mice [94]. In addition, nanobodies have exhibited applicability as tracers in magnetic resonance imaging (MRI). Small unilamellar vesicles decorated with high Gd payload (Gd-DPTA), Cy5.5, and anti-IGFBP7 were used for dual (optical and MRI) in vivo imaging of glioblastoma orthotopic models [95]. Glioblastoma immuno-PET probes based on nanobodies targeting the hepatocyte growth factor (HGF) have demonstrated diagnostic potential in preclinical models. Nanobodies 1E2 and 6E10, linked to an albumin-binding nanobody (Alb8) and labeled with the positron emitter ^{89}Zr, assessed HGF expression in xenografted glioblastoma mouse models [96]. These nanobody-based immuno-PET probes showed therapy potential as they delayed tumor growth. Other nanobody-based probes have evidenced diagnostic properties by performing MRI (R3VQ-S-(DOTA/Gd)$_3$) [97] and micro-SPECT imaging ([^{111}In]In-DTPA-pa2H [88]; ([^{111}In]In-DTPA-pa2H-Fc [98]) of Alzheimer's disease mouse models. These examples highlight the importance of the innovative field of immuno-PET tools based on the diagnostic potential of nanobodies for nuclear imaging and image-guided surgery [99].

Nanobodies have already evinced their clinical benefit in patients. In 2019, the Food and Drug Administration (FDA) and, more recently, the European Medicines Agency (EMA), approved the use of ALX-0681 (Caplacizumab; Ablynx NV, Ghent, Belgium) for adult patients with acquired thrombotic thrombocytopenic purpura [100][101]. ALX-0681 was the first nanobody

reaching the clinic field, paving the way for a new era of diagnostics and therapeutics based on nanobodies. Nanobody-derived immuno-PET tracers are advancing through clinical trials. A human epidermal growth factor receptor 2 (HER2)-targeting nanobody ([^{68}Ga]Ga-NOTA-anti-HER2 VHH1) has demonstrated its efficient diagnosis of primary breast carcinoma patients by PET/CT in a phase I study [102]. This nanobody-based tracer is being evaluated for the detection of breast-to-brain metastasis in a phase II trial (ClinicalTrials.gov NCT03331601). Recently, a phase I study was conducted to analyze the diagnostic potential of a ^{99m}Tc labeled anti-PD-L1 nanobody ([^{99m}Tc]Tc-NM-01) in non-small cell lung cancer patients by SPECT/CT imaging [103]. Nanobodies constitute a promising toolbox for innovative opportunities in the immuno-PET field towards personalized medicine.

References

1. Ostrom, Q.T.; Cioffi, G.; Waite, K.; Kruchko, C.; Barnholtz-Sloan, J.S. CBTRUS Statistical Report: Primary Brain and Other Central Nervous System Tumors Diagnosed in the United States in 2014–2018. Neuro-Oncology 2021, 23, iii1–iii105.
2. Wen, P.Y.; Santosh, K. Malignant gliomas in adults. N. Engl. J. Med. 2008, 359, 492–507.
3. Ahmed, R.; Oborski, M.J.; Hwang, M.; Lieberman, F.S.; Mountz, J.M. Malignant gliomas: Current perspectives in diagnosis, treatment, and early response assessment using advanced quantitative imaging methods. Cancer Manag. Res. 2014, 6, 149–170.
4. Verhaak, R.G.W.; Hoadley, K.A.; Purdom, E.; Wang, V.; Qi, Y.; Wilkerson, M.D.; Miller, C.R.; Ding, L.; Golub, T.; Mesirov, J.P.; et al. Integrated Genomic Analysis Identifies Clinically Relevant Subtypes of Glioblastoma Characterized by Abnormalities in PDGFRA, IDH1, EGFR, and NF1. Cancer Cell 2010, 17, 98–110.
5. Deb, P.; Sharma, M.C.; Mahapatra, A.K.; Agarwal, D.; Sarkar, C. Glioblastoma multiforme with long term survival. Neurol. India 2005, 53, 329–332.
6. Henriksson, R.; Asklund, T.; Poulsen, H.S. Impact of therapy on quality of life, neurocognitive function and their correlates in glioblastoma multiforme: A review. J. Neurooncol. 2011, 104, 639–646.
7. Stupp, R.; Hegi, M.E.; Mason, W.P.; van den Bent, M.J.; Taphoorn, M.J.; Janzer, R.C.; Ludwin, S.K.; Allgeier, A.; Fisher, B.; Belanger, K.; et al. Effects of radiotherapy with concomitant and adjuvant temozolomide versus radiotherapy alone on survival in glioblastoma in a randomised phase III study: 5-year analysis of the EORTC-NCIC trial. Lancet Oncol. 2009, 10, 459–466.
8. Esteller, M.; Garcia-Foncillas, J.; Andion, E.; Goodman, S.N.; Hidalgo, O.F.; Vanaclocha, V.; Baylin, S.B.; Herman, J.G. Inactivation of the DNA-Repair Gene MGMT and the Clinical Response of Gliomas to Alkylating Agents. N. Engl. J. Med. 2000, 349, 1350–1354.
9. Gilbert, M.R.; Wang, M.; Aldape, K.D.; Stupp, R.; Hegi, M.E.; Jaeckle, K.A.; Armstrong, T.S.; Wefel, J.S.; Won, M.; Blumenthal, D.T.; et al. Dose-dense temozolomide for newly diagnosed glioblastoma: A randomized phase III clinical trial. J. Clin. Oncol. 2013, 31, 4085–4091.
10. FDA Approves Expanded Indication for Medical Device to Treat Glioblastoma Multiforme|ESMO. Available online: https://www.esmo.org/oncology-news/archive/fda-approves-expanded-indication-for-medical-device-to-treat-glioblastoma-multiforme (accessed on 11 August 2021).
11. Fabian, D.; Eibl, M.d.P.G.P.; Alnahhas, I.; Sebastian, N.; Giglio, P.; Puduvalli, V.; Gonzalez, J.; Palmer, J.D. Treatment of glioblastoma (GBM) with the addition of tumor-treating fields (TTF): A review. Cancers 2019, 11, 174.
12. Louis, D.N.; Perry, A.; Reifenberger, G.; von Deimling, A.; Figarella-Branger, D.; Cavenee, W.K.; Ohgaki, H.; Wiestler, O.D.; Kleihues, P.; Ellison, D.W. The 2016 World Health Organization Classification of Tumors of the Central Nervous System: A summary. Acta Neuropathol. 2016, 131, 803–820.
13. Reifenberger, G.; Wirsching, H.G.; Knobbe-Thomsen, C.B.; Weller, M. Advances in the molecular genetics of gliomas-implications for classification and therapy. Nat. Rev. Clin. Oncol. 2017, 14, 434–452.
14. Louis, D.N.; Perry, A.; Wesseling, P.; Brat, D.J.; Cree, I.A.; Figarella-branger, D.; Hawkins, C.; Ng, H.K.; Pfister, S.M.; Reifenberger, G.; et al. The 2021 WHO Classification of Tumors of the Central Nervous System: A summary. Neuro-Oncology 2021, 23, 1215–1217.
15. Capper, D.; Jones, D.T.W.; Sill, M.; Hovestadt, V.; Schrimpf, D.; Sturm, D.; Koelsche, C.; Sahm, F.; Chavez, L.; Reuss, D.E.; et al. DNA methylation-based classification of central nervous system tumours. Nature 2018, 555, 469–474.
16. Brat, D.J.; Aldape, K.; Colman, H.; Holland, E.C.; Louis, D.N.; Jenkins, R.B.; Kleinschmidt-DeMasters, B.K.; Perry, A.; Reifenberger, G.; Stupp, R.; et al. cIMPACT-NOW update 3: Recommended diagnostic criteria for “Diffuse astrocytic glioma, IDH-wildtype, with molecular features of glioblastoma, WHO grade IV”. Acta Neuropathol. 2018, 136, 805–810.

17. Tesileanu, C.M.S.; Dirven, L.; Wijnenga, M.M.J.; Koekkoek, J.A.F.; Vincent, A.J.P.E.; Dubbink, H.J.; Atmodimedjo, P.N.; Kros, J.M.; Van Duinen, S.G.; Smits, M.; et al. Survival of diffuse astrocytic glioma, IDH1/2 wildtype, with molecular features of glioblastoma, WHO grade IV: A confirmation of the cIMPACT-NOW criteria. Neuro-Oncology 2020, 22, 515–523.

18. Lundy, P.; Domino, J.; Ryken, T.; Fouke, S.; McCracken, D.J.; Ormond, D.R.; Olson, J.J. The role of imaging for the management of newly diagnosed glioblastoma in adults: A systematic review and evidence-based clinical practice guideline update. J. Neurooncol. 2020, 150, 95–120.

19. Pandit-Taskar, N.; Postow, M.A.; Hellmann, M.D.; Harding, J.J.; Barker, C.A.; O'Donoghue, J.A.; Ziolkowska, M.; Ruan, S.; Lyashchenko, S.K.; Tsai, F.; et al. First-in-Humans Imaging with 89Zr-Df-IAB22M2C Anti-CD8 Minibody in Patients with Solid Malignancies: Preliminary Pharmacokinetics, Biodistribution, and Lesion Targeting. J. Nucl. Med. 2020, 61, 512–519.

20. Freise, A.C.; Wu, A.M. In vivo imaging with antibodies and engineered fragments. Mol. Immunol. 2015, 67, 142–152.

21. Kerdjoudj, R.; Pniok, M.; Alliot, C.; Kubíček, V.; Havlíčková, J.; Rösch, F.; Hermann, P.; Huclier-Markai, S. Scandium(III) complexes of monophosphorus acid DOTA analogues: A thermodynamic and radiolabelling study with 44Sc from cyclotron and from a 44Ti/44Sc generator. Dalt. Trans. 2016, 45, 1398–1409.

22. Romero, E.; Martínez, A.; Oteo, M.; Ibañez, M.; Santos, M.; Morcillo, M.Á. Development and long-term evaluation of a new 68Ge/68Ga generator based on nano-SnO2 for PET imaging. Sci. Rep. 2020, 10, 12756.

23. González-Gómez, R.; Pazo-Cid, R.A.; Sarría, L.; Morcillo, M.Á.; Schuhmacher, A.J. Diagnosis of Pancreatic Ductal Adenocarcinoma by Immuno-Positron Emission Tomography. J. Clin. Med. 2021, 10, 1151.

24. Hanahan, D.; Weinberg, R.A. Hallmarks of cancer: The next generation. Cell 2011, 144, 646–674.

25. Da Pieve, C.; Makarem, A.; Turnock, S.; Maczynska, J.; Smith, G.; Kramer-Marek, G. Thiol-reactive POds-bearing bifunctional chelators for the development of EGFR-targeting AlF-affibody conjugates. Molecules 2020, 25, 1562.

26. Lee, F.T.; Burvenich, I.J.G.; Guo, N.; Kocovski, P.; Tochon-Danguy, H.; Ackermann, U.; O'Keefe, G.J.; Gong, S.; Rigopoulos, A.; Liu, Z.; et al. l-Tyrosine Confers Residualizing Properties to a d-Amino Acid-Rich Residualizing Peptide for Radioiodination of Internalizing Antibodies. Mol. Imaging 2016, 15, 1536012116647535.

27. Chakravarty, R.; Goel, S.; Valdovinos, H.F.; Hernandez, R.; Hong, H.; Nickles, R.J.; Cai, W. Matching the decay half-life with the biological half-life: ImmunoPET imaging with44Sc-labeled Cetuximab Fab fragment. Bioconjug. Chem. 2014, 25, 2197–2204.

28. Tran, V.L.; Novell, A.; Tournier, N.; Gerstenmayer, M.; Schweitzer-Chaput, A.; Mateos, C.; Jego, B.; Bouleau, A.; Nozach, H.; Winkeler, A.; et al. Impact of blood-brain barrier permeabilization induced by ultrasound associated to microbubbles on the brain delivery and kinetics of cetuximab: An immunoPET study using 89Zr-cetuximab. J. Control. Release 2020, 328, 304–312.

29. Luo, H.; Hernandez, R.; Hong, H.; Graves, S.A.; Yang, Y.; England, C.G.; Theuer, C.P.; Nickles, R.J.; Cai, W. Noninvasive brain cancer imaging with a bispecific antibody fragment, generated via click chemistry. Proc. Natl. Acad. Sci. USA 2015, 112, 12806–12811.

30. Puttick, S.; Stringer, B.W.; Day, B.W.; Bruce, Z.C.; Ensbey, K.S.; Mardon, K.; Cowin, G.J.; Thurecht, K.J.; Whittaker, A.K.; Fay, M.; et al. EphA2 as a Diagnostic Imaging Target in Glioblastoma: A Positron Emission Tomography/Magnetic Resonance Imaging Study. Mol. Imaging 2015, 14, 385–395.

31. Sheybani, N.D.; Breza, V.R.; Paul, S.; McCauley, K.S.; Berr, S.S.; Miller, G.W.; Neumann, K.D.; Price, R.J. ImmunoPET-informed sequence for focused ultrasound-targeted mCD47 blockade controls glioma. J. Control. Release 2021, 331, 19–29.

32. Gaedicke, S.; Braun, F.; Prasad, S.; Machein, M.; Firat, E.; Hettich, M.; Gudihal, R.; Zhu, X.; Klingner, K.; Schüler, J.; et al. Noninvasive positron emission tomography and fluorescence imaging of CD133+ tumor stem cells. Proc. Natl. Acad. Sci. USA 2014, 111, E692–E701.

33. Lesniak, W.G.; Chu, C.; Jablonska, A.; Du, Y.; Pomper, M.G.; Walczak, P.; Janowski, M. A distinct advantage to intraarterial delivery of 89Zr-bevacizumab in PET imaging of mice with and without osmotic opening of the blood–brain barrier. J. Nucl. Med. 2019, 60, 617–622.

34. Liu, H.-L.; Hsu, P.-H.; Lin, C.-Y.; Huang, C.-W.; Chai, W.-Y.; Chu, P.-C.; Huang, C.-Y.; Chen, P.-Y.; Yang, L.-Y.; Kuo, J.S.; et al. Focused Ultrasound Enhances Central Nervous System Delivery of Bevacizumab for Malignant Glioma Treatment. Radiology 2016, 281, 99–108.

35. Hernandez, R.; Sun, H.; England, C.G.; Valdovinos, H.F.; Barnhart, T.E.; Yang, Y.; Cai, W. ImmunoPET imaging of CD146 expression in malignant brain tumors. Mol. Pharm. 2016, 13, 2563–2570.

36. Yang, Y.; Hernandez, R.; Rao, J.; Yin, L.; Qu, Y.; Wu, J.; England, C.G.; Graves, S.A.; Lewis, C.M.; Wang, P.; et al. Targeting CD146 with a 64Cu-labeled antibody enables in vivo immunoPET imaging of high-grade gliomas. Proc. Natl. Acad. Sci. USA 2015, 112, E6525–E6534.

37. Zhou, B.; Wang, H.; Liu, R.; Wang, M.; Deng, H.; Giglio, B.C.; Gill, P.S.; Shan, H.; Li, Z. PET Imaging of Dll4 expression in glioblastoma and colorectal cancer xenografts using 64Cu-labeled monoclonal antibody 61B. Mol. Pharm. 2015, 12, 3527–3534.

38. De Lucas, A.G.; Schuhmacher, A.J.; Oteo, M.; Romero, E.; Cámara, J.A.; de Martino, A.; Arroyo, A.G.; Morcillo, M.; Squatrito, M.; Martinez-Torrecuadrada, J.L.; et al. Targeting MT1-MMP as an immunoPET-based strategy for imaging gliomas. PLoS ONE 2016, 11, e0158634.

39. Gonzalez-Junca, A.; Reiners, O.; Borrero-Garcia, L.D.; Beckford-Vera, D.; Lazar, A.A.; Chou, W.; Braunstein, S.; VanBrocklin, H.; Franc, B.L.; Barcellos-Hoff, M.H. Positron Emission Tomography Imaging of Functional Transforming Growth Factor β (TGFβ) Activity and Benefit of TGFβ Inhibition in Irradiated Intracranial Tumors. Int. J. Radiat. Oncol. Biol. Phys. 2021, 109, 527–539.

40. Den Hollander, M.W.; Bensch, F.; Glaudemans, A.W.J.M.; Oude Munnink, T.H.; Enting, R.H.; Den Dunnen, W.F.A.; Heesters, M.A.A.M.; Kruyt, F.A.E.; Lub-De Hooge, M.N.; De Groot, J.C.; et al. TGF-β antibody uptake in recurrent high-grade glioma imaged with 89Zr-fresolimumab PET. J. Nucl. Med. 2015, 56, 1310–1314.

41. Pandya, D.N.; Sinha, A.; Yuan, H.; Mutkus, L.; Stumpf, K.; Marini, F.C.; Wadas, T.J. Imaging of fibroblast activation protein alpha expression in a preclinical mouse model of glioma using positron emission tomography. Molecules 2020, 25, 3672.

42. Molotkov, A.; Doubrovin, M.; Bhatt, N.; Hsu, F.C.; Beserra, A.; Chopra, R.; Mintz, A. 3D optical/CT as a preclinical companion imaging platform for glioblastoma drug development. Drug Deliv. 2020, 27, 1686–1694.

43. Liu, Q.; Jiang, L.; Li, K.; Li, H.; Lv, G.; Lin, J.; Qiu, L. Immuno-PET imaging of 68Ga-labeled nanobody Nb109 for dynamic monitoring the PD-L1 expression in cancers. Cancer Immunol. Immunother. 2021, 70, 1721–1733.

44. Kasten, B.B.; Houson, H.A.; Coleman, J.M.; Leavenworth, J.W.; Markert, J.M.; Wu, A.M.; Salazar, F.; Tavaré, R.; Massicano, A.V.F.; Gillespie, G.Y.; et al. Positron emission tomography imaging with 89 Zr—Labeled anti—CD8 cys—Diabody reveals—Infiltration during oncolytic virus therapy in a glioma murine model. Sci. Rep. 2021, 11, 15384.

45. Nigam, S.; McCarl, L.; Kumar, R.; Edinger, R.S.; Kurland, B.F.; Anderson, C.J.; Panigrahy, A.; Kohanbash, G.; Edwards, W.B. Preclinical ImmunoPET Imaging of Glioblastoma-Infiltrating Myeloid Cells Using Zirconium-89 Labeled Anti-CD11b Antibody. Mol. Imaging Biol. 2020, 22, 685–694.

46. Foster, A.; Nigam, S.; Tatum, D.S.; Raphael, I.; Xu, J.; Kumar, R.; Plakseychuk, E.; Latoche, J.D.; Vincze, S.; Li, B.; et al. Novel theranostic agent for PET imaging and targeted radiopharmaceutical therapy of tumour-infiltrating immune cells in glioma. EBioMedicine 2021, 71, 103571.

47. Nobashi, T.W.; Mayer, A.T.; Xiao, Z.; Chan, C.T.; Chaney, A.M.; James, M.L.; Gambhir, S.S. Whole-body PET imaging of T cell response to Glioblastoma. Clin. Cancer Res. 2021, 27, 6445–6456.

48. Quail, D.F.; Joyce, J.A. The Microenvironmental Landscape of Brain Tumors. Cancer Cell 2017, 31, 326–341.

49. Pyonteck, S.M.; Akkari, L.; Schuhmacher, A.J.; Bowman, R.L.; Sevenich, L.; Quail, D.F.; Olson, O.C.; Quick, M.L.; Huse, J.T.; Teijeiro, V.; et al. CSF-1R inhibition alters macrophage polarization and blocks glioma progression. Nat. Med. 2013, 19, 1264–1272.

50. Quail, D.F.; Bowman, R.L.; Akkari, L.; Quick, M.L.; Schuhmacher, A.J.; Huse, J.T.; Holland, E.C.; Sutton, J.C.; Joyce, J.A. The tumor microenvironment underlies acquired resistance to CSF-1R inhibition in gliomas. Science 2016, 352, aad3018.

51. Bouleau, A.; Lebon, V.; Truillet, C. PET imaging of immune checkpoint proteins in oncology. Pharmacol. Ther. 2021, 222, 107786.

52. Lu, C.T.; Zhao, Y.Z.; Wong, H.L.; Cai, J.; Peng, L.; Tian, X.Q. Current approaches to enhance CNS delivery of drugs across the brain barriers. Int. J. Nanomed. 2014, 9, 2241–2257.

53. Pardridge, W.M. Drug targeting to the brain. Pharm. Res. 2007, 24, 1733–1744.

54. Dong, X. Current strategies for brain drug delivery. Theranostics 2018, 8, 1481–1493.

55. Brasnjevic, I.; Steinbusch, H.W.M.; Schmitz, C.; Martinez-Martinez, P. Delivery of peptide and protein drugs over the blood-brain barrier. Prog. Neurobiol. 2009, 87, 212–251.

56. Levites, Y.; Smithson, L.A.; Price, R.W.; Dakin, R.S.; Yuan, B.; Sierks, M.R.; Kim, J.; McGowan, E.; Kim Reed, D.; Rosenberry, T.L.; et al. Insights into the mechanisms of action of anti-Aβ antibodies in Alzheimer’s disease mouse models. FASEB J. 2006, 20, 2576–2578.

57. Pepinsky, R.B.; Shao, Z.; Ji, B.; Wang, Q.; Meng, G.; Walus, L.; Lee, X.; Hu, Y.; Graff, C.; Garber, E.; et al. Exposure le vels of anti-LINGO-1 Li81 antibody in the central nervous system and dose-efficacy relationships in rat spinal cord remy elination models after systemic administration. J. Pharmacol. Exp. Ther. 2011, 339, 519–529.

58. Zhang, Y.; Pardridge, W.M. Rapid transferrin efflux from brain to blood across the blood-brain barrier. J. Neurochem. 20 01, 76, 1597–1600.

59. Siegelman, J.; Fleit, H.B.; Peress, N.S. Characterization of immunoglobulin G-Fe receptor activity in the outflow system of the cerebrospinal fluid. Cell Tissue Res. 1987, 248, 599–605.

60. Cooper, P.R.; Ciambrone, G.J.; Kliwinski, C.M.; Maze, E.; Johnson, L.; Li, Q.; Feng, Y.; Hornby, P.J. Efflux of monoclona l antibodies from rat brain by neonatal Fc receptor, FcRn. Brain Res. 2013, 1534, 13–21.

61. Ruano-Salguero, J.S.; Lee, K.H. Antibody transcytosis across brain endothelial-like cells occurs nonspecifically and ind ependent of FcRn. Sci. Rep. 2020, 10, 3685.

62. Salvador, J.P.; Vilaplana, L.; Marco, M.P. Nanobody: Outstanding features for diagnostic and therapeutic applications. A nal. Bioanal. Chem. 2019, 411, 1703–1713.

63. Krasniqi, A.; D'Huyvetter, M.; Devoogdt, N.; Frejd, F.Y.; Sörensen, J.; Orlova, A.; Keyaerts, M.; Tolmachev, V. Same-day imaging using small proteins: Clinical experience and translational prospects in oncology. J. Nucl. Med. 2018, 59, 885–891.

64. Širochmanová, I.; Čomor, Ľ.; Káňová, E.; Jiménez-Munguía, I.; Tkáčová, Z.; Bhide, M. Permeability of the Blood-Brain Barrier and Transport of Nanobodies Across the Blood-Brain Barrier. Folia Vet. 2018, 62, 59–66.

65. Muyldermans, S.; Baral, T.N.; Retamozzo, V.C.; De Baetselier, P.; De Genst, E.; Kinne, J.; Leonhardt, H.; Magez, S.; N guyen, V.K.; Revets, H.; et al. Camelid immunoglobulins and nanobody technology. Vet. Immunol. Immunopathol. 200 9, 128, 178–183.

66. Hamers-Casterman, C.; Atarhouch, T.; Muyldermans, S.; Robinson, G.; Hammers, C.; Songa, E.B.; Bendahman, N.; H ammers, R. Naturally occurring antibodies devoid of light chains. Nature 1993, 363, 446–448.

67. Muyldermans, S. Nanobodies: Natural single-domain antibodies. Annu. Rev. Biochem. 2013, 82, 775–797.

68. Jovčevska, I.; Muyldermans, S. The Therapeutic Potential of Nanobodies. BioDrugs 2020, 34, 11–26.

69. Steeland, S.; Vandenbroucke, R.E.; Libert, C. Nanobodies as therapeutics: Big opportunities for small antibodies. Drug Discov. Today 2016, 21, 1076–1113.

70. Jovčevska, I.; Zupanec, N.; Kočevar, N.; Cesselli, D.; Podergajs, N.; Stokin, C.L.; Myers, M.P.; Muyldermans, S.; Ghass abeh, G.H.; Motaln, H.; et al. TRIM28 and β-actin identified via nanobody-based reverse proteomics approach as possi ble human glioblastoma biomarkers. PLoS ONE 2014, 9, e113688.

71. Jovčevska, I.; Zupanec, N.; Urlep, Ž.; Vranic, A.; Matos, B.; Stokin, C.L.; Muyldermans, S.; Myers, M.P.; Buzdin, A.A.; P etrov, I.; et al. Differentially expressed proteins in glioblastoma multiforme identified with a nanobody-based anti-proteo me approach and confirmed by OncoFinder as possible tumor-class predictive biomarker candidates. Oncotarget 2017, 8, 44141–44158.

72. Van De Water, J.A.J.M.; Bagci-Onder, T.; Agarwal, A.S.; Wakimoto, H.; Roovers, R.C.; Zhu, Y.; Kasmieh, R.; Bhere, D.; Van Bergen En Henegouwen, P.M.P.; Shah, K. Therapeutic stem cells expressing variants of EGFR-specific nanobodie s have antitumor effects. Proc. Natl. Acad. Sci. USA 2012, 109, 16642–16647.

73. Samec, N.; Jovcevska, I.; Stojan, J.; Zottel, A.; Liovic, M.; Myers, M.P.; Muyldermans, S.; Šribar, J.; Križaj, I.; Komel, R. Glioblastoma-specific anti-TUFM nanobody for in-vitro immunoimaging and cancer stem cell targeting. Oncotarget 201 8, 9, 17282–17299.

74. Zottel, A.; Jovčevska, I.; Šamec, N.; Mlakar, J.; Šribar, J.; Križaj, I.; Skoblar Vidmar, M.; Komel, R. Anti-vimentin, anti-T UFM, anti-NAP1L1 and anti-DPYSL2 nanobodies display cytotoxic effect and reduce glioblastoma cell migration. Ther. Adv. Med. Oncol. 2020, 12.

75. Ruiz-López, E.; Schuhmacher, A.J. Transportation of Single-Domain Antibodies through the Blood-Brain Barrier. Biomol ecules 2021, 11, 1131.

76. Gao, Y.; Zhu, J.; Lu, H. Single domain antibody-based vectors in the delivery of biologics across the blood–brain barrie r: A review. Drug Deliv. Transl. Res. 2020, 11, 1818–1828.

77. Pothin, E.; Lesuisse, D.; Lafaye, P. Brain delivery of single-domain antibodies: A focus on VHH and VNAR. Pharmaceut ics 2020, 12, 937.

78. Bélanger, K.; Iqbal, U.; Tanha, J.; MacKenzie, R.; Moreno, M.; Stanimirovic, D. Single-Domain Antibodies as Therapeuti c and Imaging Agents for the Treatment of CNS Diseases. Antibodies 2019, 8, 27.

79. Fishman, J.B.; Rubin, J.B.; Handrahan, J.V.; Connor, J.R.; Fine, R.E. Receptor-mediated transcytosis of transferrin acr oss the blood-brain barrier. J. Neurosci. Res. 1987, 18, 299–304.

80. Fillebeen, C.; Descamps, L.; Dehouck, M.P.; Fenart, L.; Benaïssa, M.; Spik, G.; Cecchelli, R.; Pierce, A. Receptor-medi ated transcytosis of lactoferrin through the blood-brain barrier. J. Biol. Chem. 1999, 274, 7011–7017.

81. Muruganandam, A.; Tanha, J.; Narang, S.; Stanimirovic, D. Selection of phage-displayed llama single-domain antibodie s that transmigrate across human blood-brain barrier endothelium. FASEB J. 2002, 16, 240–242.

82. Abulrob, A.; Sprong, H.; Van Bergen En Henegouwen, P.; Stanimirovic, D. The blood-brain barrier transmigrating single domain antibody: Mechanisms of transport and antigenic epitopes in human brain endothelial cells. J. Neurochem. 200 5, 95, 1201–1214.

83. Farrington, G.K.; Caram-Salas, N.; Haqqani, A.S.; Brunette, E.; Eldredge, J.; Pepinsky, B.; Antognetti, G.; Baumann, E.; Ding, W.; Garber, E.; et al. A novel platform for engineering blood-brain barrier-crossing bispecific biologics. FASEB J. 2 014, 28, 4764–4778.

84. Tamai, I.; Sai, Y.; Kobayashi, H.; Kamata, M.; Wakamiya, T.; Tsuji, A. Structure-internalization relationship for adsorptive -mediated endocytosis of basic peptides at the blood-brain barrier. J. Pharmacol. Exp. Ther. 1997, 280, 410–415.

85. Hervé, F.; Ghinea, N.; Scherrmann, J.M. CNS delivery via adsorptive transcytosis. AAPS J. 2008, 10, 455–472.

86. Li, T.; Bourgeois, J.P.; Celli, S.; Glacial, F.; Le Sourd, A.M.; Mecheri, S.; Weksler, B.; Romero, I.; Couraud, P.O.; Rougeo n, F.; et al. Cell-penetrating anti-GFAP VHH and corresponding fluorescent fusion protein VHH-GFP spontaneously cro ss the blood-brain barrier and specifically recognize astrocytes: Application to brain imaging. FASEB J. 2012, 26, 3969 –3979.

87. Li, T.; Vandesquille, M.; Koukouli, F.; Dudeffant, C.; Youssef, I.; Lenormand, P.; Ganneau, C.; Maskos, U.; Czech, C.; Gr ueninger, F.; et al. Camelid single-domain antibodies: A versatile tool for in vivo imaging of extracellular and intracellular brain targets. J. Control. Release 2016, 243, 1–10.

88. Rotman, M.; Welling, M.M.; Bunschoten, A.; De Backer, M.E.; Rip, J.; Nabuurs, R.J.A.; Gaillard, P.J.; Van Buchem, M. A.; Van Der Maarel, S.M.; Van Der Weerd, L. Enhanced glutathione PEGylated liposomal brain delivery of an anti-amyl oid single domain antibody fragment in a mouse model for Alzheimer's disease. J. Control. Release 2015, 203, 40–50.

89. van Lith, S.A.M.; van den Brand, D.; Wallbrecher, R.; van Duijnhoven, S.M.J.; Brock, R.; Leenders, W.P.J. A Conjugate of an Anti-Epidermal Growth Factor Receptor (EGFR) VHH and a Cell-Penetrating Peptide Drives Receptor Internalizat ion and Blocks EGFR Activation. ChemBioChem 2017, 18, 2390–2394.

90. Yin, W.; Zhao, Y.; Kang, X.; Zhao, P.; Fu, X.; Mo, X.; Wan, Y.; Huang, Y. BBB-penetrating codelivery liposomes treat bra in metastasis of non-small cell lung cancer with EGFRT790M mutation. Theranostics 2020, 10, 6122–6135.

91. Chakravarty, R.; Goel, S.; Cai, W. Nanobody: The "magic bullet" for molecular imaging? Theranostics 2014, 4, 386–39 8.

92. Iqbal, U.; Trojahn, U.; Albaghdadi, H.; Zhang, J.; O'Connor-Mccourt, M.; Stanimirovic, D.; Tomanek, B.; Sutherland, G.; Abulrob, A. Kinetic analysis of novel mono- and multivalent VHH-fragments and their application for molecular imaging of brain tumours: RESEARCH PAPER. Br. J. Pharmacol. 2010, 160, 1016–1028.

93. Fatehi, D.; Baral, T.N.; Abulrob, A. In vivo imaging of brain cancer using epidermal growth factor single domain antibody bioconjugated to near-infrared quantum dots. J. Nanosci. Nanotechnol. 2014, 14, 5355–5362.

94. Iqbal, U.; Albaghdadi, H.; Luo, Y.; Arbabi, M.; Desvaux, C.; Veres, T.; Stanimirovic, D.; Abulrob, A. Molecular imaging of glioblastoma multiforme using anti-insulin-like growth factor-binding protein-7 single-domain antibodies. Br. J. Cancer 2 010, 103, 1606–1616.

95. Iqbal, U.; Albaghdadi, H.; Nieh, M.P.; Tuor, U.I.; Mester, Z.; Stanimirovic, D.; Katsaras, J.; Abulrob, A. Small unilamellar vesicles: A platform technology for molecular imaging of brain tumors. Nanotechnology 2011, 22, 195102.

96. Vosjan, M.J.W.D.; Vercammen, J.; Kolkman, J.A.; Stigter-Van Walsum, M.; Revets, H.; Van Dongen, G.A.M.S. Nanobo dies targeting the hepatocyte growth factor: Potential new drugs for molecular cancer therapy. Mol. Cancer Ther. 2012, 11, 1017–1025.

97. Vandesquille, M.; Li, T.; Po, C.; Ganneau, C.; Lenormand, P.; Dudeffant, C.; Czech, C.; Grueninger, F.; Duyckaerts, C.; Delatour, B.; et al. Chemically-defined camelid antibody bioconjugate for the magnetic resonance imaging of Alzheime r's disease. mAbs 2017, 9, 1016–1027.

98. Rotman, M.; Welling, M.M.; van den Boogaard, M.L.; Moursel, L.G.; van der Graaf, L.M.; van Buchem, M.A.; van der M aarel, S.M.; van der Weerd, L. Fusion of hIgG1-Fc to 111In-anti-amyloid single domain antibody fragment VHH-pa2H p rolongs blood residential time in APP/PS1 mice but does not increase brain uptake. Nucl. Med. Biol. 2015, 42, 695–70 2.

99. Debie, P.; Devoogdt, N.; Hernot, S. Targeted Nanobody-Based Molecular Tracers for Nuclear Imaging and Image-Guided Surgery. Antibodies 2019, 8, 12.
100. Duggan, S. Caplacizumab: First Global Approval. Drugs 2018, 78, 1639–1642.
101. Scully, M.; Cataland, S.R.; Peyvandi, F.; Coppo, P.; Knöbl, P.; Kremer Hovinga, J.A.; Metjian, A.; de la Rubia, J.; Pavenski, K.; Callewaert, F.; et al. Caplacizumab Treatment for Acquired Thrombotic Thrombocytopenic Purpura. N. Engl. J. Med. 2019, 380, 335–346.
102. Keyaerts, M.; Xavier, C.; Heemskerk, J.; Devoogdt, N.; Everaert, H.; Ackaert, C.; Vanhoeij, M.; Duhoux, F.P.; Gevaert, T.; Simon, P.; et al. Phase I study of 68Ga-HER2-Nanobody for PET/CT assessment of HER2 expression in breast carcinoma. J. Nucl. Med. 2016, 57, 27–33.
103. Xing, Y.; Chand, G.; Liu, C.; Cook, G.J.R.; O'Doherty, J.; Zhao, L.; Wong, N.C.L.; Meszaros, L.K.; Ting, H.H.; Zhao, J. Early phase I study of a 99mTc-labeled anti-programmed death ligand-1 (PD-L1) single-domain antibody in SPECT/CT assessment of PD-L1 expression in non-small cell lung cancer. J. Nucl. Med. 2019, 60, 1213–1220.